

This is a repository copy of *Molecular fossils as a tool for tracking Holocene sea-level change in the Loch of Stenness, Orkney*.

White Rose Research Online URL for this paper:

<https://eprints.whiterose.ac.uk/164615/>

Version: Published Version

Article:

Conti, Martina L.G., Bates, Martin R., Preece, Richard C. et al. (2 more authors) (2020) Molecular fossils as a tool for tracking Holocene sea-level change in the Loch of Stenness, Orkney. *Journal of Quaternary Science*. pp. 881-891. ISSN 0267-8179

<https://doi.org/10.1002/jqs.3238>

Reuse

This article is distributed under the terms of the Creative Commons Attribution (CC BY) licence. This licence allows you to distribute, remix, tweak, and build upon the work, even commercially, as long as you credit the authors for the original work. More information and the full terms of the licence here:

<https://creativecommons.org/licenses/>

Takedown

If you consider content in White Rose Research Online to be in breach of UK law, please notify us by emailing eprints@whiterose.ac.uk including the URL of the record and the reason for the withdrawal request.

Molecular fossils as a tool for tracking Holocene sea-level change in the Loch of Stenness, Orkney

MARTINA L. G. CONTI,¹  MARTIN R. BATES,²  RICHARD C. PREECE,³ KIRSTY E. H. PENKMAN¹  and BRENDAN J. KEELY^{1*} 

¹Department of Chemistry, University of York, Heslington, York, UK

²Faculty of Humanities and Performing Arts, University of Wales Trinity Saint David, Lampeter, Ceredigion, Wales, UK

³Department of Zoology, University of Cambridge, Downing Street, Cambridge, UK

Received 19 December 2019; Revised 26 July 2020; Accepted 29 July 2020

ABSTRACT: Sediments deposited in the Loch of Stenness (Orkney Islands, Scotland) during the Holocene transgression, previously dated to between ~5939–5612 BP, were analysed for molecular fossils – lipids and chlorophyll pigments from primary producers – that complement conventional microfossil and lithological approaches for studying past sea-level change. While microfossil and lithological studies identified a transgression between 102 and 81 cm core depth, key molecular fossils fluctuate in occurrence and concentration between 118 and 85 cm, suggesting an earlier start to the transgression. Terrestrial lipid concentrations decreased and algal-derived, short-chain, *n*-alkanoic acid concentrations increased at 118 cm, indicating a disruption of the freshwater lake conditions associated with the early stages of the marine transgression. The lipid and pigment analyses provided information that complements and extends that from microfossil analysis, presenting a more complete record of Holocene sea-level changes and local vegetation changes in the Loch of Stenness. The isostatic stability of Stenness during the Holocene points towards other factors to explain the transgression, such as regional factors and/or melting of the Antarctic ice sheet (which occurred up to 3 ka).

© 2020 The Authors. *Journal of Quaternary Science* Published by John Wiley & Sons Ltd.

KEYWORDS: chlorophylls; Holocene; lipids; molecular fossils; sea level

Introduction

Changes in sea level have been studied extensively to understand their causes and impacts on the environment and human populations (Rollins *et al.*, 1979; Hodgson *et al.*, 2009; Bates *et al.*, 2016; IPCC, 2019). By understanding the main drivers and consequences of past sea-level changes, this knowledge can be applied to understanding future climate and sea-level change scenarios on local and global scales (Church *et al.*, 2008).

Transgressions and regressions can lead to changes in the dominance of terrestrial or marine sources of organic matter (OM) at a particular location. Nutrient availability, degradation of OM and sedimentation rates can also be affected to different extents, strongly depending on the basin topography. The changes in water depth inherent in a transgression may lead to changes in sedimentation and in the extent of sediment reworking (Cattaneo and Steel, 2003). During a regression, nutrient input may decrease, thus reducing productivity and sedimentation of OM (Cattaneo and Steel, 2003). Localized fluctuations between terrestrial- and marine-dominated conditions in coastal/near coastal regions can be inferred from seismic mapping, palaeontological analysis, changes in the nature and morphology of the sediments, and changes in the composition and nature of OM (Shennan *et al.*, 2015). Environmental proxies for tracking transgressions based on soil and sediment analysis exploit shifts in the populations of plant macrofossils, insects, pollen and spores, foraminifera,

diatoms, molluscs and ostracods (Horton *et al.*, 1992; Bunting, 1994; Davis *et al.*, 2003; Bates *et al.*, 2016).

While a major challenge in using macro- and microfossil evidence is their extent of preservation and/or limited number of specimens, it is often possible to extract organic geochemical molecular fossils incorporated into the sediment matrix. Through their relationship to the biological molecules from which they originate, the molecular fossils can reflect specific OM inputs (Fig. 1) and thereby reveal characteristics of, and changes in, the environment inhabited by the source organisms (Poynter and Eglinton, 1990; Meyers and Ishiwatari, 1993; Castañeda and Schouten, 2011). Molecular fossils can be analysed within milligram to gram quantities of sediment, a much smaller scale than the few grams needed for traditional macro- and microfossil analyses (Shennan *et al.*, 2015). Hence, sampling resolution can be reduced, even to millimetre scale where justifiable, enabling analyses at higher temporal resolution (Airs and Keely, 2002). Robust lithological and morphological studies are key to identifying the areas of undisturbed sediments that are ideal for palaeoenvironmental and molecular fossil analyses, avoiding compromised areas (e.g. where bioturbation or burrowing has occurred).

Molecular fossils inferring sea-level changes

The widespread occurrence of molecular fossils in sediments and their derivation from both aquatic and terrestrial sources allows the recognition of allochthonous and autochthonous sources of OM in sediments (Eglinton and Hamilton, 1967; Cranwell, 1982; Keely, 2006). Extensive research on the diagenetic transformation of various biomarkers enables reconstructions based on the principal molecular fossils of

*Correspondence: B. Keely or M. Conti, as above.

E-mails: brendan.keely@york.ac.uk; martina.conti@alumni.york.ac.uk

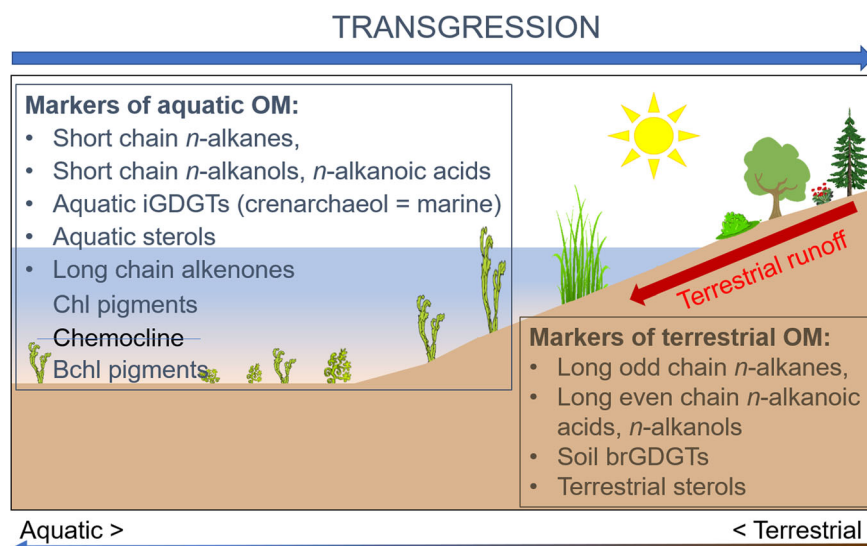


Figure 1. Summary of key biological markers used in this study and their association with particular organic matter sources. Abbreviations: OM = organic matter; iGDGTs = isoprenoid glycerol dialkyl glycerol tetraethers; Chl = chlorophyll pigments; Bchl = bacteriochlorophyll pigments; brGDGTs = branched glycerol dialkyl glycerol tetraethers. [Color figure can be viewed at wileyonlinelibrary.com]

primary producers, such as chlorophyll pigments, *n*-alkanes, alcohols, fatty acids and tetraether lipids (Eglinton and Hamilton, 1967; Harradine *et al.*, 1996; Airs *et al.*, 2001; Volkman, 2005; Schouten *et al.*, 2013). However, the use of molecular fossils to identify and study sea-level fluctuations has been largely overlooked with only a few studies reported in the literature (e.g. Ficken and Farrimond, 1995; Squier *et al.*, 2002; Bendle *et al.*, 2009; van Soelen *et al.*, 2010; Carr *et al.*, 2015; De Jonge *et al.*, 2016; Li *et al.*, 2017). The combined use of several molecular fossils is key to identifying sea-level changes (Fig. 1). It can be expected that a transgression will result in a shift in the molecular fossil assemblage from mostly terrestrial OM (from either land runoff or *in situ* production) to a more significant marine contribution (Fig. 1).

Terrestrial OM reflects the vegetation in the hinterland through the distributions of: sterols that occur widely in higher plants (Volkman, 1986), long odd-chain *n*-alkanes (*n*-C_{25–35}) and long even-chain *n*-alkanols and *n*-alkanoic acids (*n*-C_{22–30}) prominent in higher plant waxes (Cranwell, 1973, 1982). Furthermore, branched glycerol dialkyl glycerol tetraether lipids (brGDGTs), structural cores of the polar membrane lipids of eubacteria, represent soil microbial communities (Fig. 1; Schouten *et al.*, 2013). By contrast, aquatic conditions are represented by isoprenoid GDGTs (iGDGTs), derivatives of the structural membrane lipids of commonly occurring Archaea (Schouten *et al.*, 2013). Among these, crenarchaeol is a specific marker for marine Archaea (Damsté *et al.*, 2002). Although low level production of iGDGTs in soil and some brGDGTs in aquatic environments has been noted (DeLong, 1992; DeLong *et al.*, 1994; Hershberger *et al.*, 1996; Tierney and Russell, 2009; Fietz *et al.*, 2012; Li *et al.*, 2016), the general source distinction between the two groups is employed widely for tracing the origin and transport patterns of soil OM (Sun *et al.*, 2011; Doğrul Selver *et al.*, 2012; Zhu *et al.*, 2013). Other markers of aquatic conditions include short-chain-length *n*-alkanes (*n*-C_{17–24}), common in bacteria and algae (Cranwell, 1973), and predominance of short even-chain *n*-alkanols and *n*-alkanoic acids (*n*-C₁₆, *n*-C₁₈), although these also occur in some plants (Meyers and Ishiwatari, 1993). Long-chain unsaturated alkenones (*n*-C_{37–39}) are common markers of haptophyte algae in marine sediments, especially C_{37:3} and C_{37:2} (Marlowe *et al.*, 1984). In coastal as well as freshwater and saline lake systems, C_{37:4} occurs alongside C_{37:3} and C_{37:2} (Cranwell, 1985; Bendle *et al.*, 2009; Table 1).

Changes in molecular fossil distribution correlate with changes in environmental conditions, giving rise to proxies that reflect the origins of OM, water temperature and soil pH. Specific proxies, indicators of palaeoenvironmental conditions, have been sug-

gested to distinguish inputs of plant OM (average chain length, ACL; Poynter and Eglinton, 1990), terrestrial from marine OM based on brGDGTs and crenarchaeol (branched and isoprenoid tetraether index, BIT; Hopmans *et al.*, 2004), and terrestrial from freshwater OM based on *n*-alkane carbon chain lengths (proxy of aquatic macrophytes, P_{aq}; Ficken *et al.*, 2000; Table 1). In immature sediments, the carbon preference index (CPI; Bray and Evans, 1961) can reflect predominance of either terrestrial or algal OM (Clark and Blumer, 1967; Ortiz *et al.*, 2004; Table 1). The tetraether index of 86 carbons (TEX₈₆; Schouten *et al.*, 2002; Table 1), based on iGDGTs, is a proxy for sea-surface water temperature (SST), and mean annual air temperature (MAAT) can be reconstructed from the methylation of branched tetraethers (MBT; Weijers *et al.*, 2007). A proxy proposed to reconstruct soil pH is based on brGDGTs (cyclization of branched tetraethers, CBT; Weijers *et al.*, 2007; Table 1). Other proxies for temperature estimations exist but are not applied in this work; for example, U₃₇^k is based on long-chain alkenones (Brassell *et al.*, 1986; Prahl and Wakeham, 1987) and RAN₁₃, RAN₁₅ and RAN₁₇ on 3-OH fatty acids (Wang *et al.*, 2016; Yang *et al.*, 2020).

Changes in the availability of nutrients in aquatic environments can be reflected by fluctuations in the concentrations of particular chlorophyll pigments (broadly described as chlorins) produced by the photosynthetic organisms inhabiting the water column (Fig. 1; Keely, 2006). The physicochemical conditions in the water column are reflected by particular pigment structures. Photoautotrophs that live in oxygen-rich waters, including aquatic plants, photosynthetic algae and cyanobacteria, produce chlorophyll pigments (chls; Scheer, 1991). By contrast, bacteriochlorophylls (bchls) are the photoreceptors in the purple and green bacteria, which are restricted to anoxic waters (Fig. 1; Pfennig, 1977). Covariance in organic carbon and chlorin accumulation provides evidence that pigment concentrations reflect changes in productivity, for example, during glacial/interglacial cycles (Harris *et al.*, 1996). Short-term transgressions can be evident in changes in the nature and distribution of chlorophyll pigments (Squier *et al.*, 2002; Hodgson *et al.*, 2009).

Aims

There is considerable potential for routinely using molecular fossils for sea-level studies. In the UK, Holocene transgressive sequences have been extensively studied in many of the larger estuaries and coastal environments in England (Devoy, 1977; Long *et al.*, 2000; Sidell, 2003; Bates and Stafford, 2013) and Scotland (Long *et al.*, 2016; Palamakumbura, 2018). In most cases, however, the precise nature and duration of the flooding

Table 1. Proxies developed from biological markers of terrestrial, freshwater and marine organic matter (OM).

Proxy	What it represents	Markers	Values and inference	References
Carbon preference index (CPI)	Extent of input of fresh terrestrial and algal OM	Long chain <i>n</i> -alkanes $n\text{-C}_{23-33}$	>5: fresh terrestrial OM <5: algal OM	Bray and Evans (1961)
Proxy for aquatic macrophytes (P_{aq})	Ratio used to discriminate between higher plant and freshwater macrophyte OM	Long odd chain <i>n</i> -alkanes $n\text{-C}_{23}$, $n\text{-C}_{25}$, $n\text{-C}_{29}$, $n\text{-C}_{31}$	<0.1: terrestrial plants 0.1–0.4: emergent macrophytes 0.4–1: submerged/floating macrophytes	Ficken <i>et al.</i> (2000)
Average chain length (ACL)	Average carbon number of terrestrial plants	<i>n</i> -alkanes $n\text{-C}_{27}$, $n\text{-C}_{29}$ and $n\text{-C}_{31}$	Predominance $n\text{-C}_{27}$: forest Predominance $n\text{-C}_{31}$: grasses	Cranwell (1973); Poynter and Eglinton (1990)
Branched and isoprenoid tetraether (BIT)	Ratio that discriminates terrestrial runoff from marine OM	brGDGTs and crenarchaeol	0: marine OM 1: terrestrial OM	Hopmans <i>et al.</i> (2004)
Tetraether index of 86 carbon atoms (TEX_{86})	Reconstruction of sea-surface temperature	iGDGTs, including crenarchaeol stereoisomer	Sea-surface water temperature in °C	Schouten <i>et al.</i> (2002)
Lake temperature	Lake water temperature	brGDGTs	Lake-water temperature in °C	Pearson <i>et al.</i> (2011)
Cyclization of branched tetraethers (CBT)	Reconstruction of soil pH	brGDGTs	pH values	Weijers <i>et al.</i> (2007)

event remains difficult to determine. Sea-level index points from Scottish sites show sea-level fluctuations (~12–3 ka) resulting from glacio-eustasy and isostasy, subsequently approaching present-day levels (~3 ka to present; Shennan, 1989; Shennan and Horton, 2002; Selby and Smith, 2007). The timing of the fluctuations in the Mid–Late Holocene varies regionally; for example, Orkney sea-level approached present values ~5–4 ka BP (Shennan and Horton, 2002). Seismic and palaeoenvironmental analyses of a series of Late Glacial to Holocene sediment cores from the Loch of Stenness, Orkney, demonstrated the impact of the transgression on the local geography and how it might have impacted human settlement (Bates *et al.*, 2016).

Building on the existing research on sea-level change at the Loch of Stenness, the overall aim of this study was to use this well-constrained transgression record to develop a complementary method to study sea-level change using molecular fossils, largely overlooked in sea-level studies. Analysis of a combination of molecular fossils could provide a valuable record of marine and terrestrial OM inputs and changes associated with the transgression. This approach has the potential to provide more detailed and explicit environmental records of the impact of the transgression on sedimentary OM, allowing better constraints on the timing of events.

Materials and methods

Site description

The Loch of Stenness is an ~4-km-long brackish lake situated in the main island of the Orkney archipelago, Scotland (Fig. 2a), and connected to the sea at the Brig O'Waithe (Fig. 2b). The area has been inhabited since at least 3500 BC (~5.5 ka); the extensive archaeological evidence forms part of the Heart of Neolithic Orkney World Heritage Site (Farrell *et al.*, 2014).

Previous studies of the Loch of Stenness Core 2014-1

The core lithology (Core 2014-1; Fig. 2c) consists of a grey–brown organic silt with mollusc shells between 200 and 141 cm core depth, overlain by a pale grey silt with occasional shell fragments (141–81.5 cm). The uppermost sediments (81.5–0 cm) comprise soft, dark grey silt with occasional shell fragments of brackish species. The loss-on-ignition profile (Fig. 3) indicates that the organic component was >20% below 140 cm depth and between 10 and 17% above 140 cm depth; higher values are associated with the coarsest sediments of the core. Carbonate-rich sediments below 85.5 cm (10–26%) and seismic layering are associated with slower sedimentation and controlled deposition in a freshwater environment (Bates *et al.*, 2016).

Palaeoenvironmental reconstruction, inferred from foraminifera, mollusc and ostracod assemblages, suggests two main environmental settings: a freshwater coastal lake (200 and 104 cm) and a brackish loch (102 and 20 cm). The brackish environment was further subdivided on the basis of the microfossil fauna: 102–81 cm shows onset of tidal access under very low brackish conditions (mix of brackish and freshwater ostracods) and 80–0 cm represents a brackish environment in which decalcification occurred and a restricted foraminiferal assemblage existed (Supporting Information, Table S1; Bates *et al.*, 2016).

Radiocarbon dating of *Lymnaea* sp. shells at 92–94 cm and at 82–84 cm showed that the incursion began between ~5939 and 5753 BP and was fully established between ~5862 and 5612 BP (Table S2; Bates *et al.*, 2016).

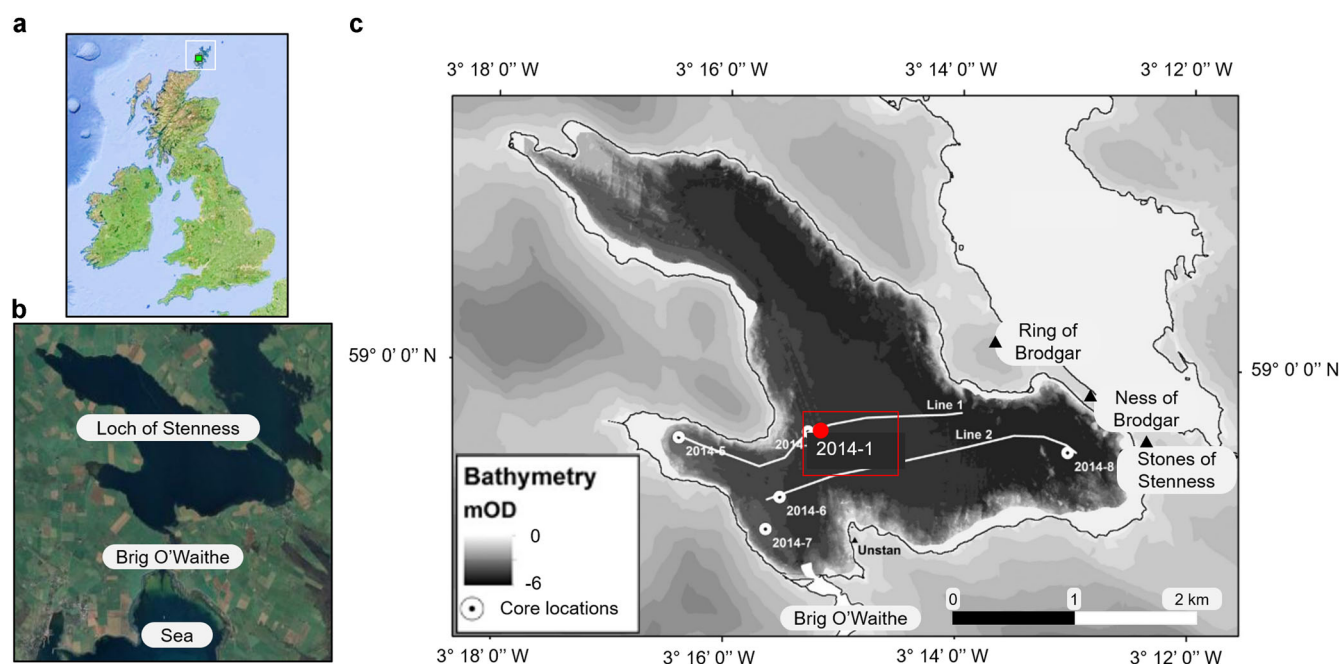


Figure 2. (a) Map of the British Isles showing the Orkney archipelago (white square) and the Loch of Stenness (green square; adapted from Google Maps); (b) map of the Loch of Stenness showing the Brig O'Waithe and the connection to the sea (adapted from Google Maps); (c) map of the Loch of Stenness showing the location of Core 2014-1 in the red rectangle. Bathymetry only shown for the Loch of Stenness (adapted from Bates *et al.*, 2016). [Color figure can be viewed at wileyonlinelibrary.com]

Separation of mollusc shells

The freeze-dried sediment was inspected for intact gastropod shells before grinding and sieving. Any shells found were removed with a spatula and/or forceps and sonicated in deionized water to remove sediment residues. The species were identified after air-drying in a fumehood overnight.

Extraction and analysis of molecular fossils

For complete methods, see Table S3. The core was subsampled at 10 depths (Fig. 3). The freeze-dried sediment was homogenized and sieved (Saesaengseerung, 2013). Extraction of OM from this fraction was carried out using accelerated solvent extraction (Schouten *et al.*, 2007; Saesaengseer-

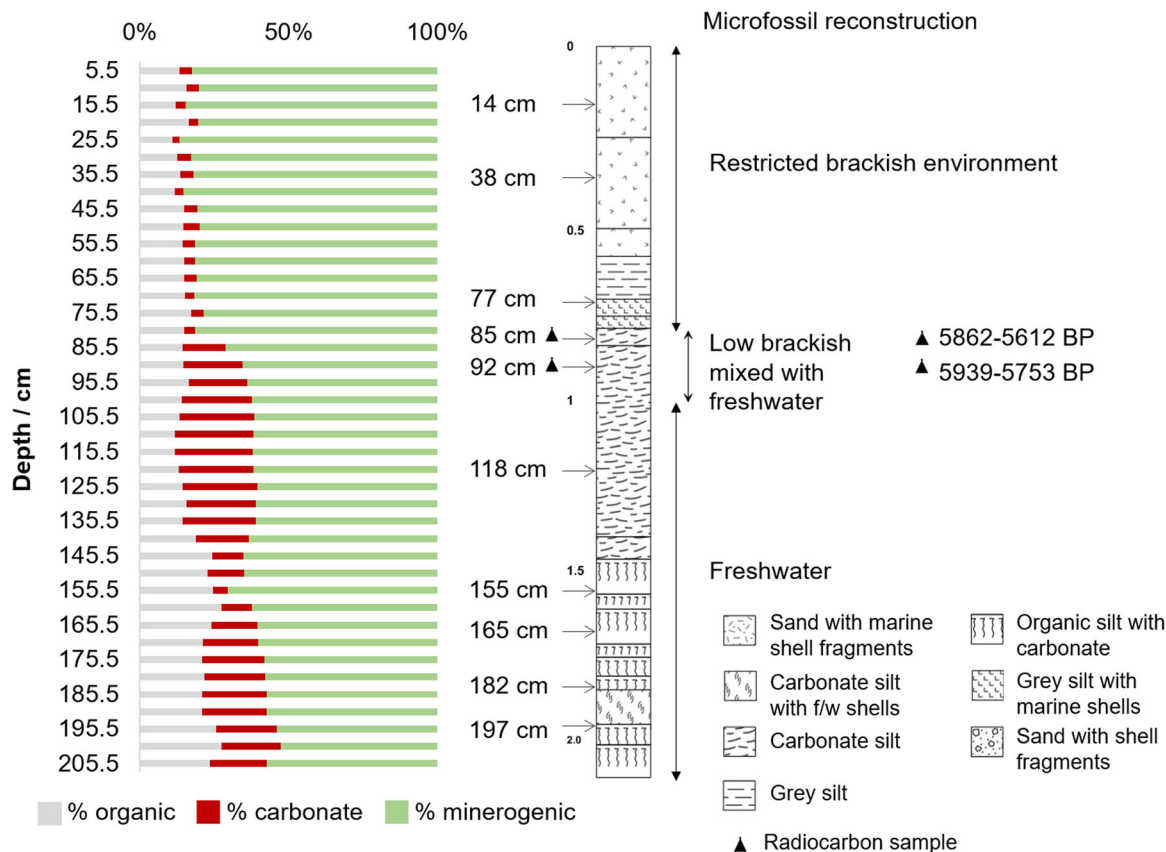


Figure 3. Stenness Core 2014-1 showing the main lithological zones, the loss-on-ignition results (sampled every 5 cm) and the dates of the beginning and end of transgression according to Bates *et al.* (2016); sampling depths analysed in this study are marked with arrows. [Color figure can be viewed at wileyonlinelibrary.com]

Table 2. Depth ranges (cm) of key environmental transitions identified by Bates *et al.* (2016) in the core from the Loch of Stenness, and the depths subsampled here for molecular fossil analysis.

Identified zone	Bates <i>et al.</i> (2016)	This study
Brackish loch	80–0	77, 38, 14
Onset tidal access	102–81	92, 85
Freshwater coastal lake	200–104	197, 182, 165, 155, 118

ung, 2013). The lipids were separated into four distinct polarity fractions using flash column chromatography (Green, 2013). These fractions were analysed by high-performance liquid chromatography with mass spectrometry (HPLC-MS of GDGTs; Schouten *et al.*, 2007) and by gas chromatography-flame ionization detection (GC-FID) and selected samples by GC with mass spectrometry (GC-MS; Green, 2013). Following extraction, chlorophyll pigments were analysed by ultra-high performance liquid chromatography with diode array detector (UHPLC-DAD) and UHPLC-MS (Saesaengseerung, 2013).

Results and discussion

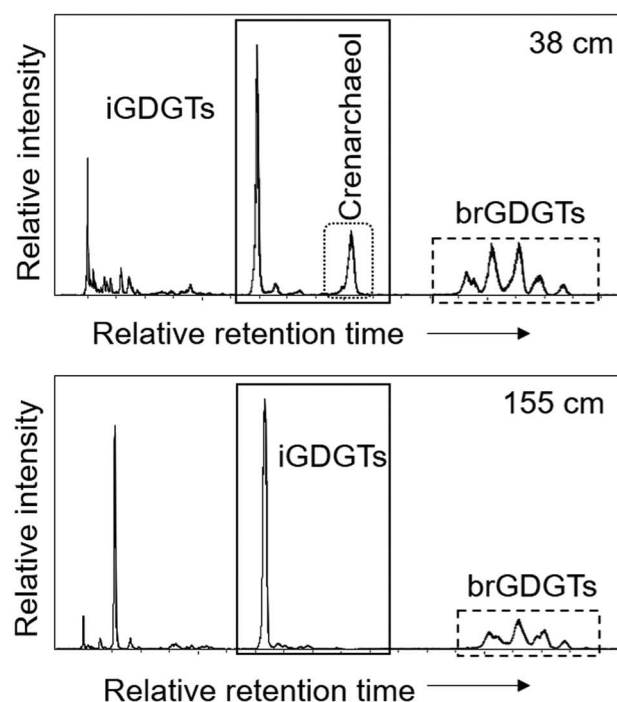
Shells of the freshwater gastropods *Gyraulus crista*, *Gyraulus laevis* and *Radix balthica* were identified between 197 and 85 cm depth, supporting the findings of Bates *et al.* (2016) who identified predominantly freshwater ostracods with some brackish species between 200 and 81 cm (Table S1). The following sections build on the interpretation of Bates *et al.* (2016), that the core sequence represents a freshwater lake (200–104 cm), the onset of brackish conditions (102–81 cm) and the formation of a brackish loch (80–0 cm), reporting molecular fossil data from these critical horizons (Table 2).

The freshwater lake (200–104 cm)

The predominance of brGDGTs and absence of marine marker crenarchaeol confirmed a freshwater lake environment in the lowest part of the core (Figs 4 and 5a; Table 3), with a prevalence of terrestrial OM input from runoff. The input of terrestrial OM was revealed by the occurrence of long odd-chain *n*-alkanes (Fig. 6a) and high CPI values (Fig. 5b; Table 3). The prevalence of terrestrial OM was further indicated by a dominance of long even-chain *n*-alkanols and *n*-alkanoic acids (Fig. 6b; Cranwell, 1982; Meyers and Ishiwatari, 1993), long odd-chain *n*-alkanes (Fig. 6a; Bray and Evans, 1961; Cranwell, 1973) together with stigmasterol and β -sitosterol, the major sterols of higher plants (the latter also an abundant component in emergent water plants; Fig. 6c; Meyers and Ishiwatari, 1993). Further evidence of terrestrial input comes from the presence of the sterol obtusifolol of *Sphagnum* moss and vascular plant origins (Fig. 6c; Ronkainen *et al.*, 2013). Although brGDGTs can have terrestrial and minor aquatic sources, the dominance of other plant/terrestrial markers suggests input from soils. Mixed terrestrial and emergent macrophyte origins for the *n*-alkanes, consistent with a permanent body of water during the freshwater stage, was evident by the occurrence of markers both for higher plant waxes and for freshwater macrophytes, reflected in the P_{aq} index values (Fig. 5c; Table 3; Ficken *et al.*, 2000). Evidence for an aquatic OM contribution from Archaea, algae and/or bacteria comes from small amounts of iGDGTs (Fig. 4; Powers *et al.*, 2010; Bischoff *et al.*, 2016; De Jonge *et al.*, 2016) and from short-chain *n*-alkanoic acids occurring above 182 cm (Fig. 6b; Cranwell, 1982).

Notably, at 118 cm there is a change in the OM: algal markers become the dominant components, reflecting a relative reduction in terrestrial deposition and increase in algal OM production, possibly enhanced by increased preservation resulting from water column anoxia (Fig. 6a,b,d). This observation probably indicates the disruption of the freshwater lake conditions associated with the early stages of the marine transgression identified from the microfossil assemblage at 102 cm (Bates *et al.*, 2016).

Detail on the water column conditions was provided by the chl and bchl pigments. As is commonly observed, intact and early diagenetic transformation products (formed via enzymatic, herbivore grazing and oxidative processes) were incorporated into the sediment (Fig. S1; Shuman and Lorenzen, 1975; Hendry *et al.*, 1987; Harradine *et al.*, 1996; Ma and Dolphin, 1996; Walker *et al.*, 2002; Keely, 2006). The fluctuations in the summed concentrations of chl and bchl pigments implies short-term changes in primary production (Fig. 6d). At 197 cm the predominance of chl pigments indicates a fully oxidized water column. The presence of bacterioviridin *a* (bvir *a*), an oxidation product of bchl *a* (Wilson *et al.*, 2004), suggests either a shallow-water environment with significant fluctuations in oxygenation or that desiccation occurred at this time. Core depths between 182 and 118 cm record a mixed primary producer community with the dominant oxygenic population separated from a deeper anoxygenic population by a chemocline (Pfennig, 1977; Gervais, 1998). Chemoclines form in zones of oxygen depletion and reducing environments (Pfennig, 1977). The presence of a fully developed chemocline and absence of bvir *a* from 182 to 118 cm indicates that the OM was not affected by fluctuations in oxygenation, suggesting that the water column was deeper than at 197 cm.

**Figure 4.** HPLC-MS chromatograms *m/z* 950–1500 of GDGTs from the Loch of Stenness from depths of 38 cm (top) and 155 cm (bottom). The boxes indicate iGDGTs (solid line), brGDGTs (dashed line) and crenarchaeol (dotted line). Note presence of the marine marker crenarchaeol at 38 cm.

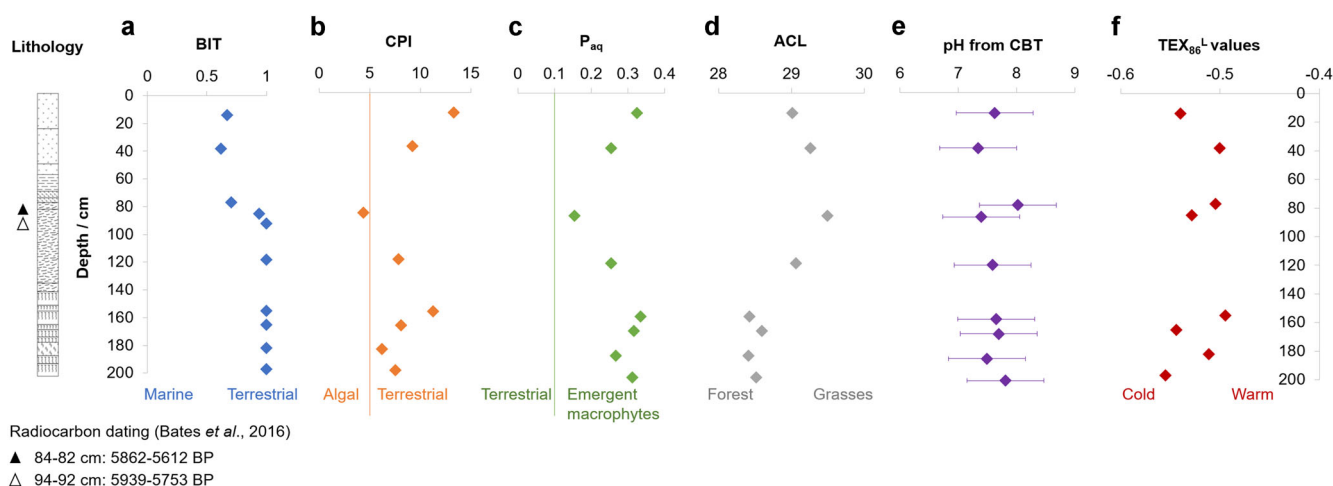


Figure 5. Lithology and radiocarbon dating from Bates *et al.* (2016), and proxies applied to the Loch of Stenness sediments: (a) BIT (branched and isoprenoid tetraether lipids); (b) CPI (carbon preference index based on *n*-alkanes); (c) P_{aq} (proxy of aquatic macrophytes based on *n*-alkanes); (d) ACL (average chain length based on *n*-alkanes); (e) pH calculated from CBT (cyclization of branched tetraether lipids); (f) TEX_{86}^L values (tetraether index of 86 carbons – low) for sea-surface temperature calculations. [Color figure can be viewed at [wileyonlinelibrary.com](https://onlinelibrary.wiley.com)]

Table 3. CPI, P_{aq} , ACL and BIT indices, pigment and sterol evidence, TEX_{86}^L values and sea surface temperatures (SST) calculated from TEX_{86}^L , and mean summer lake temperature for the Loch of Stenness sediments.

Depth (cm)	CPI [†] terrestrial vs. algal ^a	P_{aq} [‡] terrestrial vs. freshwater ^a	ACL* grass vs. forest ^a	BIT [§] terrestrial vs marine	Pigments ^c	Sterols ^d	TEX_{86}^L values ^{¶b}	SST from TEX_{86}^L (°C ± 4.0) ^b	Summer lake water temperature [‡] (°C ± 2.1) ^b
14	13.3	0.32	29.0	0.71	n.d.		−0.54	10.5	
38	9.20	0.25	29.3	0.62	n.d.		−0.51	13.1	
77	n.d.	n.d.	n.d.	0.55	n.d.		−0.50	12.8	
85	4.39	0.15	29.5	0.95	Oxic		−0.53		
92	n.d.	n.d.	n.d.	1	Low production	n.d.	n.d.		
118	7.85	0.25	29.1	1	Chemocline		n.d.		18.6
155	11.3	0.33	28.4	1			−0.49		21.0
165	8.09	0.32	28.6	1			−0.54		21.4
182	6.23	0.27	28.4	1			−0.51		20.5
197	7.56	0.31	28.5	1	Shallow water		−0.55		21.4

^a *n*-alkanes below detection limit precluded the calculation of CPI, P_{aq} , and ACL.

^b Key iGDGTs below detection limit precluded the calculation of SST from TEX_{86}^L and/or mean summer lake water temperature.

^c No pigments detected.

^d Sterols below detection limit.

: terrestrial OM; : aquatic OM; : marine OM; : mixed origin of OM; : grass; : forest.

Water temperature: **warm water**, **cold water**.

[†] CPI: carbon preference index (Supplementary Information, Table S4).

[‡] P_{aq} : proxy for aquatic macrophytes (Table S4).

* ACL: average chain length (Table S4).

[§] BIT: branched and isoprenoid tetraether index (Table S4).

[¶] TEX_{86}^L : tetraether index of 86 carbon atoms (low) (Table S4).

[‡] Mean summer lake water temperature (Table S4).

Note: absolute values are probably not appropriate, but the general trend is likely to be indicative of palaeoenvironmental change.

n.d.: not determined because below the detection limit.

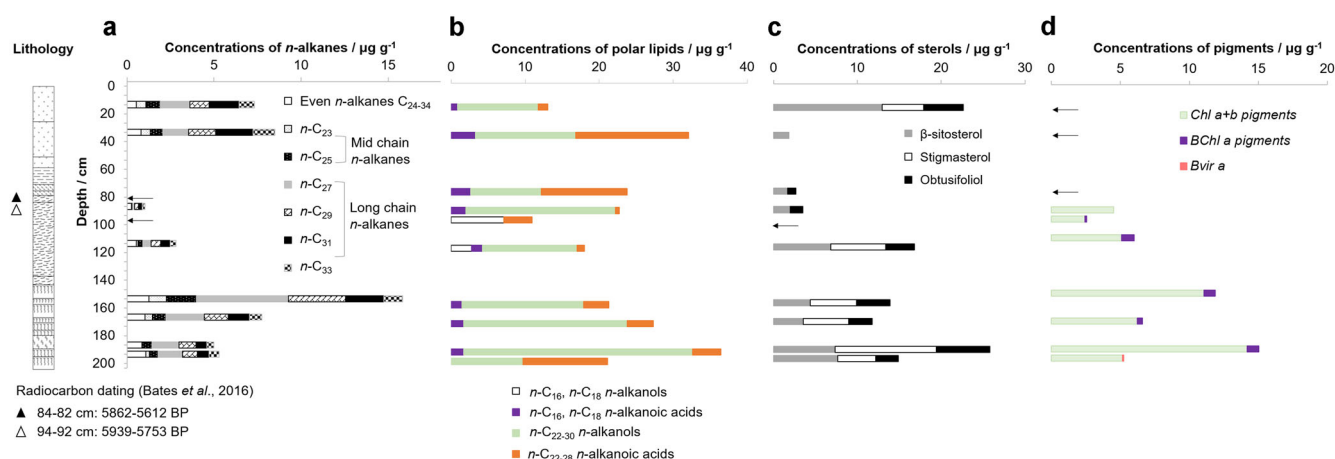


Figure 6. Lithology and radiocarbon dating from Bates *et al.* (2016), and: (a) concentrations of *n*-alkanes *n*- C_{23-35} ; (b) concentrations of *n*- C_{16} , *n*- C_{18} and *n*- C_{22-30} *n*-alkanols, and *n*- C_{16} , *n*- C_{18} and *n*- C_{22-28} *n*-alkanoic acids; (c) concentrations of sterols; (d) total concentrations of chlorophyll *a+b*, bacteriochlorophyll *a* pigments and bacterioviridin *a* in the Loch of Stenness sediments. Arrows indicate sample depths where lipids or pigments were not detected. [Color figure can be viewed at wileyonlinelibrary.com]

The marine transgression (102–81 cm)

At 92 cm core depth (94–92 cm, 5939–5753 ^{14}C a BP; Bates *et al.*, 2016) signatures of *n*-alkanes were absent/below the detection limit. An increasing dominance of aquatic OM (algal *n*-alkanols) at the expense of terrestrial OM reflects the continuation of the marine transgression (Fig. 6a–c). A much reduced population of anaerobic photosynthetic organisms probably reflects disruption of the chemocline (Fig. 6d).

At 85 cm (84–82 cm, 5862–5612 ^{14}C a BP; Bates *et al.*, 2016), a low CPI value of 4.39 (Fig. 5b; Table 3) was recorded. This can indicate a dilution in the terrestrial OM by algal *n*-alkanes, even though concentrations are low, as shown by the *n*-alkane profile (Fig. 6a; Clark and Blumer, 1967; Ortiz *et al.*, 2004). The presence of algal OM is also confirmed by short-chain *n*-alkanoic acids and pigments. The low P_{aq} proxy indicates enhanced terrestrial OM input and a decrease in freshwater macrophytes compared with the samples in earlier horizons (Fig. 5c; Table 3; Ficken *et al.*, 2000).

While microfossil evidence indicates brackish conditions being established from 102 cm, the detection of crenarchaeol at 85 cm depth indicates the onset of production by a small population of marine Thaumarchaeota (Figs 4 and 5a; Table 3). The contrast with other lipid analyses that suggest that the freshwater lake was disrupted from as early as 118 cm could reflect a lag in the production of Thaumarchaeota with them only becoming prominent once stable brackish conditions became established towards the end of the transgression.

The absence of bchls at 85 cm reveals the disappearance of the chemocline with establishment of a fully oxic water column (Fig. 6d). Such a shift in the primary producer community can result from turbulence in the water column (Squier *et al.*, 2002). It is evident that the sample at 85 cm represents a switch between a turbulent environment (from the pigments) and a stable environment (from the GDGTs) representing the ongoing transgressive event.

The established brackish loch (80–0 cm)

Established marine production with terrestrial OM input is indicated by the presence of crenarchaeol and soil brGDGTs (77–14 cm; Fig. 4). The range of BIT values observed is comparable to open coastal environments (Fig. 5a; Table 3; Hopmans *et al.*, 2004; Doğrul Selver *et al.*, 2012). The *n*-alkanol and *n*-alkanoic acid distributions and concentrations indicate a dominance of terrestrial over aquatic OM (Fig. 6b).

The similarity of the lipid concentrations to those preserved in the freshwater lake environment is consistent with cessation of the disruption associated with the transgression (Figs 5 and 6). The high CPI values throughout the brackish loch section confirm the predominance of terrestrial OM and lower contribution from algal OM (Fig. 5b; Table 3). The absence of chl pigments in this section of the core is consistent with strongly oxidative conditions leading to total destruction of pigments (Fig. 6d; Hendry *et al.*, 1987).

Signatures of terrestrial vegetation as markers of changing environment

The higher plant-derived *n*-alkanes show a shift in chain length with depth, the maximum changing from *n*- C_{27} (197–155 cm) to *n*- C_{31} (from 85 cm; Fig. 6a), reflected in the lower ACL values between 197 and 155 cm and higher values above 85 cm (Fig. 5d; Table 3; Poynter and Eglinton, 1990). Such a shift in the predominance of *n*-alkane chain lengths has been suggested to reflect a change in the surrounding vegetation from mainly forest vegetation (dominant *n*- C_{27}) to mainly grasses (dominant *n*- C_{31} ; Cranwell, 1973; Ortiz *et al.*, 2004). This would imply that the Stenness catchment area experienced gradual deforestation from the freshwater period (before ~5939–5753 BP) with grassland dominating after inundation (~5862–5612 BP). This observation provides a tantalizing view of the changing environment and should be a stimulus for further work that could involve identification of more specific grass/forest biomarkers, palynological studies and modelling to gain further insights into the palaeoclimatic conditions (Fisher *et al.*, 2003; Zech *et al.*, 2013; Li *et al.*, 2018).

Palynological analysis of a core from Crudale Meadow, located ~5 km north-west of the Loch of Stenness, suggests a predominance of arboreal pollen (AP) mainly *Betula* and *Pinus sylvestris* with <15% herbs, between 8.1 and 5.7 ka BP (Bunting, 1994). A decline in AP to 40% and increase in herbs and Filicales (ferns) are apparent from 5.7 to 4.7 ka BP, and a predominance of herbaceous taxa (Cyperaceae and Poaceae >75%) between 4.7 ka BP and today (Bunting, 1994). Similar results were obtained from Blows Moss, ~40 km south of the Loch of Stenness site (Farrell *et al.*, 2014).

The vegetation change is thought to have resulted from a cooling climate and human activity in the surrounding area (Keatinge and Dickson, 1979; Bunting, 1994; Farrell *et al.*, 2014; Bates *et al.*, 2016). The decrease in AP at Crudale Meadow by 5.7–4.7 ka BP coincides with the end of the Loch of

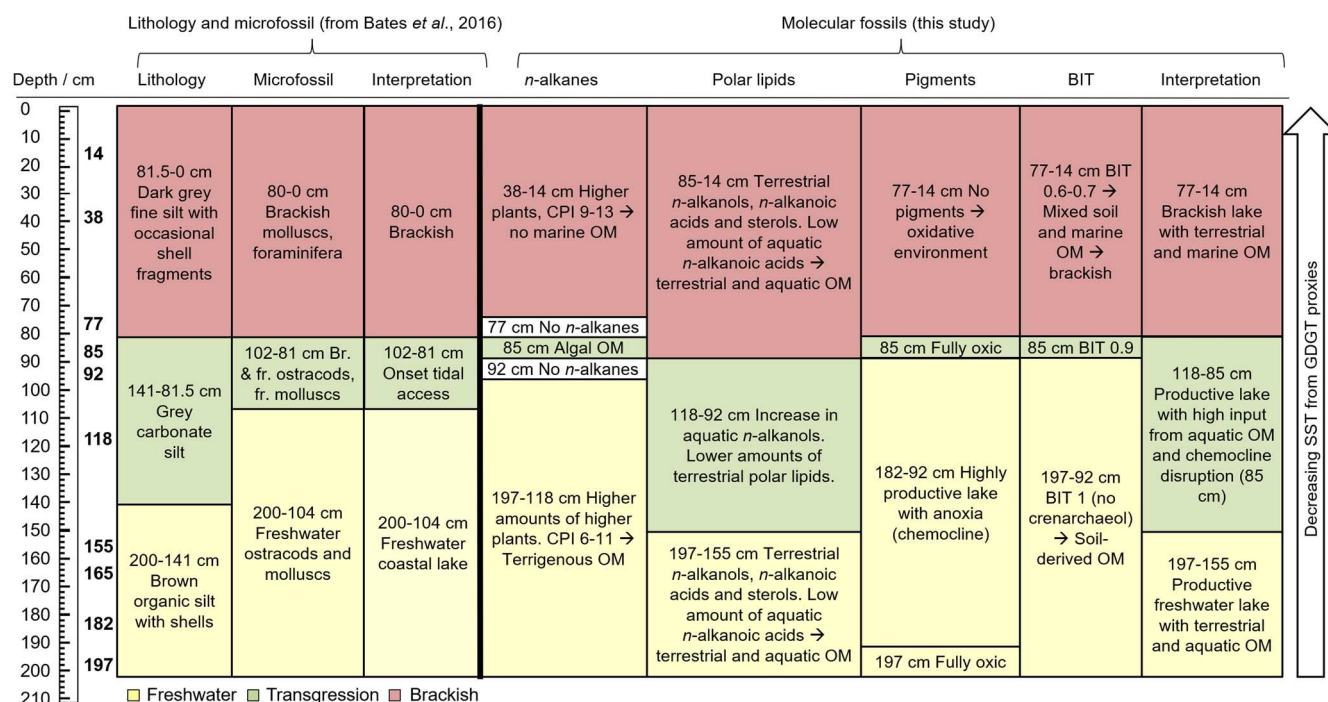


Figure 7. Scheme summarizing the main findings from the core from the Loch of Stenness, Orkney: lithology, microscopy, *n*-alkanes, polar lipids, pigments, BIT index and interpretation. [Color figure can be viewed at [wileyonlinelibrary.com](https://onlinelibrary.wiley.com)]

Stenness transgression and the observed shift towards longer chain *n*-alkanes indicative of grassland dominance (~5862–5612 BP). Thus, the combination of these two independent sources of evidence provides a compelling indication of a local change in vegetation from forest to grassland cover.

Water temperature and pH from GDGT-based indices

The pollen data from Crudale Meadow suggested that climate cooling coinciding with the transgression was partly responsible for the shift from arboreal to grass vegetation (Bunting, 1994). SST estimates could not be inferred from the TEX₈₆ index (Schouten *et al.*, 2002; Table S4) or lake temperature index (Powers *et al.*, 2010) due to lack of the crenarchaeol stereoisomer, a component that is essential to the index (note: the former assignment as regioisomer has been superseded; Damsté *et al.*, 2018). Lack of all components precluded the estimation of MAAT via the MBT index (Weijers *et al.*, 2007). The alternative TEX₈₆^L proxy for SST (Table S4) does not include the crenarchaeol stereoisomer and performs best in subpolar marine settings (below 15 °C, such as northern Scotland; Kim *et al.*, 2010). Therefore, the TEX₈₆^L calibration was applied to the brackish samples (77–14 cm) and showed low TEX₈₆^L values (Fig. 5f), indicating low SST ranging from 10.5 to 13.1 °C, ± 4 °C (Table 3). Notably, in this setting where the proxy should be most accurate, SSTs are remarkably similar to the present-day average SST of Orkney, ranging from 7.1 °C in March to 13.2 °C in August, giving an average yearly temperature of 10.1 °C (<https://www.seatemperature.org/europe/united-kingdom/orkney.htm>).

A proxy developed for freshwater lake sediments based on brGDGTs (Pearson *et al.*, 2011; Table S4) was applied to the freshwater samples (from 197 to 118 cm). The results show a reconstructed summer lake temperature of 18.6–21.4 °C. The calculated temperatures in the Loch of Stenness, however, should not be considered as absolute values, in recognition that BIT > 0.5 and the use of two GDGT palaeothermometers. A shift in the archaeal and bacterial populations and/or a

possible contribution of archaeal GDGTs produced in sediments could also account for the observed temperature change. The general trends, however, are likely to indicate changing environmental conditions. The two methods of reconstructing temperatures imply a general cooling of the lake water during and after the seawater incursion. This trend is reflected in the Mid–Late Holocene inundation by cool marine waters that coincided with a period of reduced summer insolation (Wanner *et al.*, 2008). A temperature decline was identified for this period in the North Atlantic (Wanner *et al.*, 2008) using the U^k₃₇ proxy. Mean summer air temperatures estimated from analysis of chironomids from Scotland were consistent with declining summer insolation during the Mid–Late Holocene (1.5–2 °C; Dalton *et al.*, 2005).

Structural variations in brGDGTs have been correlated with soil pH, via the CBT index (Weijers *et al.*, 2007). The applicability to lake sediments was established via a modification of the calibration (Tierney *et al.*, 2010; Table S4). The CBT-calculated pH values show a narrow range of mildly alkaline sediments between 7.34 and 8.02 ± 0.66 (Fig. 5e), values consistent with the geology of the area (Kellock, 1969).

Contextualizing the transgression

North-eastern Scotland experienced a positive isostatic rebound of +0.53 mm a⁻¹ over the last 6000 years BP (Shennan, 1989) and Orkney experienced a rebound of <0.0 mm a⁻¹ over the last 4000 years BP (Shennan and Horton, 2002; de la Vega-Leinert *et al.*, 2007).

The transgression at the Loch of Stenness cannot be attributed to melting of the Orkney island ice sheet, which occurred much earlier, between 16.0 and 14.8 ka (Ballantyne, 2010). By contrast, modelling shows that the Antarctic Ice Sheet continued to thin until at least 6 ka (Mauz *et al.*, 2015), and in some cases until 3 ka (Hein *et al.*, 2016; Small *et al.*, 2019), and has been invoked to explain the Mid–Late Holocene sea-level increase in sites across the globe (Mauz *et al.*, 2015). Notably, however, during the Mid–Late Holocene, sea-level fluctuations at Scottish sites have shown

both transgressions and regressions, indicating that regional factors, such as crustal movements and tidal dynamics (Smith *et al.*, 2019) cannot be excluded. Indeed, local factors such as the natural creation and destruction/modification of bay mouth barriers (lying ~ 5 m OD in the Loch of Stenness) are likely to have played an important role in the timing and nature of transgressions in the Loch of Stenness (Bates *et al.*, 2016). Shennan and Horton (2002) suggested that Orkney sea levels reached present values 5–4 ka, in agreement with the radiocarbon dates for this core (Bates *et al.*, 2016) and the present study on the Loch of Stenness.

Conclusions

The analysis of microfossils from the Loch of Stenness (Orkney) core reveals initial freshwater conditions (200–104 cm depth), followed by a transgression (102–81 cm) leading to brackish conditions (80–0 cm; Bates *et al.*, 2016). The molecular fossil record indicates greater complexity during the transgression than had been apparent from palaeoecological records alone. The initial freshwater lake was a productive environment with input both from *in situ* aquatic production and from terrestrial runoff (197–155 cm). The first indication of a disruption of the OM balance was recorded at 118 cm, where terrestrial OM decreased and algal OM increased in concentration, possibly indicating an earlier initiation of the transgression than is evident from microfossil analysis (Bates *et al.*, 2016). An increase in aquatic OM production was observed at 92 cm with the marine marker crenarchaeol being detected above 85 cm, consistent with the establishment of stable marine conditions (Fig. 7). In the brackish zone (77–14 cm) marine OM was detected and the extent of terrestrial runoff was similar to that of the freshwater stage, indicating the end of the transgression.

The change in *n*-alkane chain lengths and ACL values suggest a shift in vegetation from forest to grasses towards the top of the core, supported by pollen data, probably in response to cooling conditions associated with reduced summer insolation as well as human activity. The proxy-calculated SST suggests a cooling trend towards values close to present-day water temperatures at 77, 38 and 14 cm (13.1–10.5 °C, ± 4 °C).

Piloted on a well-constrained Holocene transgression, this study has shown that molecular fossils can add valuable environmental evidence to the information garnered from more conventional estimates of palaeoclimate change from microfossil, palynological and lithological studies. The nature and specific origins of molecular fossils enable a more insightful and refined study of the impact of the transgression on the primary producers inhabiting the basin and the surrounding environment. The widespread nature, greater frequency of occurrence and excellent preservation potential of molecular fossils broadens the scope of palaeoenvironmental studies and unlocks a far wider set of sediments that can be used in the study of sea-level change across the world, including sediments where macro- and microfossils are lacking.

Supporting information

Additional supporting information may be found in the online version of this article at the publisher's web-site.

Table S1. Lithological and microfossil analysis from Loch of Stenness (Orkney, Scotland) core 2014-1.

Table S2. Radiocarbon data from the Loch of Stenness (adapted from Bates *et al.*, 2016).

Table S3. Extended methods for the extraction and analysis of molecular fossils employed in this study.

Table S4. Equations for *n*-alkane-based proxies CPI, ACL and P_{aq} , GDGT-based proxies BIT, TEX_{86} , TEX_{86}^L , mean summer lake water temperature and CBT. Structures of GDGTs discussed in the table are included.

Figure S1. Concentrations of chlorophyll pigments in the Loch of Stenness core 2014-1: chlorophyllone (chlone), phaeophytin a (phe a), pyropheophytin a (pphe a), pyropheophorbide a (pphorb a), hydroxyphaeophytin a (hphe a), purpurin-7 trimethyl ester, chlorin e6, phaeophytin b (phe b), bacteriochlorophyll a (bchl a), bacteriopheophytin a (bphe a), pyrobacteriopheophytin (bpphe a), and bacterioviridin a (bvir a).

Acknowledgements. We thank the Centre of Excellence in Mass Spectrometry for the use of the APCI-MS and GC-MS and the Chemistry Department Teaching Laboratories for the use of the GC-FID (University of York, York). M.L.G.C. was funded by a Department of Chemistry teaching studentship.

Data availability statement

The data that support the findings of this study are available from the corresponding authors upon reasonable request.

Abbreviations. ACL, average chain length; AP, arboreal pollen; bchl, bacteriochlorophyll; BIT, branched and isoprenoid tetraether; brGDGT, branched glycerol dialkyl glycerol tetraether; bvir a, bacterioviridin a; CBT, cyclization of branched tetraethers; chl, chlorophyll; CPI, carbon preference index; GC-FID, gas chromatography-flame ionization detection; GC-MS, gas chromatography-mass spectrometry; GDGT, glycerol dialkyl glycerol tetraether; iGDGT, isoprenoid GDGT; MAAT, mean annual air temperature; OM, organic matter; SST, sea-surface temperature; UHPLC-DAD, ultra-high performance liquid chromatography with diode array detector.

References

- Airs RL, Atkinson JE, Keely BJ. 2001. Development and application of a high resolution liquid chromatographic method for the analysis of complex pigment distributions. *Journal of Chromatography. A* **917**: 167–177.
- Airs RL, Keely BJ. 2002. Atmospheric pressure chemical ionisation liquid chromatography/mass spectrometry of bacteriochlorophylls from Chlorobiaceae: characteristic fragmentations. *Rapid Communications in Mass Spectrometry* **16**: 453–461.
- Ballantyne CK. 2010. Extent and deglacial chronology of the last British–Irish ice sheet: implications of exposure dating using cosmogenic isotopes. *Journal of Quaternary Science* **25**: 515–534.
- Bates CR, Bates MR, Dawson S *et al.* 2016. The environmental context of the Neolithic monuments on the Brodgar Isthmus, Mainland, Orkney. *Journal of Archaeological Science: Reports* **7**: 394–407.
- Bates MR, Stafford E, Slater, G & Anderson-Whymark, H. 2013. *Thames Holocene: A Geoarchaeological Approach to the Investigation of the River Floodplain for High Speed 1, 1994–2003*. Oxford Wessex Archaeology: Salisbury.
- Bendle JAP, Rosell-Melé A, Cox NJ *et al.* 2009. Alkenones, alkenoates, and organic matter in coastal environments of NW Scotland: assessment of potential application for sea level reconstruction. *Geochemistry, Geophysics, Geosystems* **10**.
- Bischoff J, Sparkes RB, Doğrul Selver A *et al.* 2016. Source, transport and fate of soil organic matter inferred from microbial biomarker lipids on the East Siberian Arctic Shelf. *Biogeosciences* **13**: 4899–4914.
- Brassell SC, Eglinton G, Marlowe IT *et al.* 1986. Molecular stratigraphy: a new tool for climatic assessment. *Nature* **320**: 129–133.
- Bray EE, Evans ED. 1961. Distribution of *n*-paraffins as a clue to recognition of source beds. *Geochimica et Cosmochimica Acta* **22**: 2–15.
- Bunting MJ. 1994. Vegetation history of Orkney, Scotland; pollen records from two small basins in west Mainland. *New Phytologist* **128**: 771–792.

- Carr AS, Boom A, Chase BM *et al.* 2015. Holocene sea level and environmental change on the west coast of South Africa: evidence from plant biomarkers, stable isotopes and pollen. *Journal of Paleolimnology* **53**: 415–432.
- Castañeda IS, Schouten SA. 2011. A review of molecular organic proxies for examining modern and ancient lacustrine environments. *Quaternary Science Reviews* **30**: 2851–2891.
- Cattaneo A, Steel RJ. 2003. Transgressive deposits: a review of their variability. *Earth-Science Reviews* **62**: 187–228.
- Church JA, White NJ, Aarup T *et al.* 2008. Understanding global sea levels: past, present and future. *Sustainability Science* **3**: 9–22.
- Clark RC Jr., Blumer M. 1967. Distribution of *n*-paraffins in marine organisms and sediment. *Limnology and Oceanography* **12**: 79–87.
- Cranwell PA. 1973. Chain-length distribution of *n*-alkanes from lake sediments in relation to post-glacial environmental change. *Freshwater Biology* **3**: 259–265.
- Cranwell PA. 1982. Lipids of aquatic sediments and sedimenting particulates. *Progress in Lipid Research* **21**: 271–308.
- Cranwell PA. 1985. Long-chain unsaturated ketones in recent lacustrine sediments. *Geochimica et Cosmochimica Acta* **49**: 1545–1551.
- Dalton C, Birks HJB, Brooks SJ *et al.* 2005. A multi-proxy study of lake-development in response to catchment changes during the Holocene at Lochnagar, north-east Scotland. *Palaeogeography, Palaeoclimatology, Palaeoecology* **221**: 175–201.
- Damsté JSS, Schouten S, Hopmans EC *et al.* 2002. Crenarchaeol: the characteristic core glycerol dibiphytanyl glycerol tetraether membrane lipid of cosmopolitan pelagic Crenarchaeota. *Journal of Lipid Research* **43**: 1641–1651.
- Damsté JSS, Rijpstra WIC, Hopmans EC *et al.* 2018. The enigmatic structure of the crenarchaeol isomer. *Organic Geochemistry* **124**: 22–28.
- Davis BAS, Brewer S, Stevenson AC *et al.* 2003. The temperature of Europe during the Holocene reconstructed from pollen data. *Quaternary Science Reviews* **22**: 1701–1716.
- De Jonge C, Stadnitskaia A, Cherkashov G *et al.* 2016. Branched glycerol dialkyl glycerol tetraethers and crenarchaeol record post-glacial sea level rise and shift in source of terrigenous brGDGTs in the Kara Sea (Arctic Ocean). *Organic Geochemistry* **92**: 42–54.
- de la Vega-Leinert AC, Smith DE, Jones RL. 2007. Holocene coastal environmental changes on the periphery of an area of glacio-isostatic uplift: an example from Scapa Bay, Orkney, UK. *Journal of Quaternary Science* **22**: 755–772.
- DeLong EF. 1992. Archaea in coastal marine environments. *Proceedings of the National Academy of Sciences of the United States of America* **89**: 5685–5689.
- DeLong EF, Wu KY, Prézelin BB *et al.* 1994. High abundance of Archaea in Antarctic marine picoplankton. *Nature* **371**: 695–697.
- Devoy RJN. 1977. Flandrian sealevel changes in the Thames Estuary and the implications for land subsidence in England and Wales. *Nature* **270**: 712–715.
- Doğrul Selver A, Talbot HM, Gustafsson Ö *et al.* 2012. Soil organic matter transport along a sub-arctic river–sea transect. *Organic Geochemistry* **51**: 63–72.
- Eglinton G, Hamilton RJ. 1967. Leaf epicuticular waxes. *Science* **156**: 1322–1335.
- Farrell M, Bunting MJ, Lee DHJ *et al.* 2014. Neolithic settlement at the woodland's edge: palynological data and timber architecture in Orkney, Scotland. *Journal of Archaeological Science* **51**: 225–236.
- Ficken KJ, Farrimond P. 1995. Sedimentary lipid geochemistry of Framvaren: impacts of a changing environment. *Marine Chemistry* **51**: 31–43.
- Ficken KJ, Li B, Swain DL *et al.* 2000. An *n*-alkane proxy for the sedimentary input of submerged/floating freshwater aquatic macrophytes. *Organic Geochemistry* **31**: 745–749.
- Fietz S, Huguet C, Bendle J *et al.* 2012. Co-variation of crenarchaeol and branched GDGTs in globally distributed marine and freshwater sedimentary archives. *Global and Planetary Change* **92–93**: 275–285.
- Fisher E, Oldfield F, Wake R *et al.* 2003. Molecular marker records of land use change. *Organic Geochemistry* **34**: 105–119.
- Gervais F. 1998. Ecology of cryptophytes coexisting near a freshwater chemocline. *Freshwater Biology* **39**: 61–78.
- Green KA. 2013. *The fate of lipids in archaeological burial soils* PhD Thesis, University of York.
- Harradine PJ, Harris PG, Head RN *et al.* 1996. Steryl chlorin esters are formed by zooplankton herbivory. *Geochimica et Cosmochimica Acta* **60**: 2265–2270.
- Harris PG, Zhao M, Rosell-Melé A *et al.* 1996. Chlorin accumulation rate as a proxy for Quaternary marine primary productivity. *Nature* **383**: 63–65.
- Hein AS, Marrero SM, Woodward J *et al.* 2016. Mid-Holocene pulse of thinning in the Weddell Sea sector of the West Antarctic ice sheet. *Nature Communications* **7**: 12511.
- Hendry GAF, Houghton JD, Brown SB. 1987. The degradation of chlorophyll: a biological enigma. *New Phytologist* **107**: 255–302.
- Hershberger KL, Barns SM, Reysenbach AL *et al.* 1996. Wide diversity of Crenarchaeota. *Nature* **384**: 420.
- Hodgson DA, Verleyen E, Vyverman W *et al.* 2009. A geological constraint on relative sea level in Marine Isotope Stage 3 in the Larsemann Hills, Lambert Glacier region, East Antarctica (31 366–33 228 cal yr BP). *Quaternary Science Reviews* **28**: 2689–2696.
- Hopmans EC, Weijers JWH, Schefuß E *et al.* 2004. A novel proxy for terrestrial organic matter in sediments based on branched and isoprenoid tetraether lipids. *Earth and Planetary Science Letters* **224**: 107–116.
- Horton A, Keen DH, Field MH *et al.* 1992. The Hoxnian–Interglacial deposits at Woodston, Peterborough. *Philosophical Transactions of the Royal Society of London. Series B* **338**: 131–164.
- IPCC. 2019. Technical Summary. In IPCC Special Report on the Ocean and Cryosphere in a Changing Climate, Pörtner H-O, Roberts DC, Masson-Delmotte V (eds). IPCC; 37–69.
- Keatinge TH, Dickson JH. 1979. Mid-Flandrian changes in vegetation on Mainland Orkney. *New Phytologist* **82**: 585–612.
- Keely BJ. 2006. Geochemistry of chlorophylls, *Chlorophylls and Bacteriochlorophylls*. Springer: Berlin; 535–561.
- Kellock E. 1969. Alkaline basic igneous rocks in the Orkneys. *Scottish Journal of Geology* **5**: 140–153.
- Kim JH, van der Meer J, Schouten S *et al.* 2010. New indices and calibrations derived from the distribution of crenarchaeal isoprenoid tetraether lipids: implications for past sea surface temperature reconstructions. *Geochimica et Cosmochimica Acta* **74**: 4639–4654.
- Li J, Pancost RD, Naafs BDA *et al.* 2016. Distribution of glycerol dialkyl glycerol tetraether (GDGT) lipids in a hypersaline lake system. *Organic Geochemistry* **99**: 113–124.
- Li X, Anderson BJ, Vogeler I *et al.* 2018. Long-chain *n*-alkane and *n*-fatty acid characteristics in plants and soil – potential to separate plant growth forms, primary and secondary grasslands? *Science of the Total Environment* **645**: 1567–1578.
- Li X, Zong Y, Zheng Z *et al.* 2017. Marine deposition and sea surface temperature changes during the last and present interglacials in the west coast of Taiwan Strait. *Quaternary International* **440**: 91–101.
- Long AJ, Barlow NLM, Dawson S *et al.* 2016. Lateglacial and Holocene relative sea-level changes and first evidence for the Storegga tsunami in Sutherland, Scotland. *Journal of Quaternary Science* **31**: 239–255.
- Long AJ, Scaife RG, Edwards RJ. 2000. Stratigraphic architecture, relative sea-level, and models of estuary development in southern England: new data from Southampton Water. *Geological Society, London, Special Publications* **175**: 253–279.
- Ma L, Dolphin D. 1996. Stereoselective synthesis of new chlorophyll a related antioxidants isolated from marine organisms. *Journal of Organic Chemistry* **61**: 2501–2510.
- Marlowe IT, Green JC, Neal AC *et al.* 1984. Long chain (*n*-C₃₇–C₃₉) alkenones in the Prymnesiophyceae. Distribution of alkenones and other lipids and their taxonomic significance. *British Phycological Journal* **19**: 203–216.
- Mauz B, Ruggieri G, Spada G. 2015. Terminal Antarctic melting inferred from a far-field coastal site. *Quaternary Science Reviews* **116**: 122–132.
- Meyers PA, Ishiwatari R. 1993. Lacustrine organic geochemistry – an overview of indicators of organic matter sources and diagenesis in lake sediments. *Organic Geochemistry* **20**: 867–900.
- Ortiz JE, Torres T, Delgado A *et al.* 2004. The palaeoenvironmental and palaeohydrological evolution of Padul Peat Bog (Granada, Spain) over one million years, from elemental, isotopic and molecular organic geochemical proxies. *Organic Geochemistry* **35**: 1243–1260.

- Palamakumbura R. 2018. A new palaeogeographic model for the post-glacial marine and estuarine sediments of the Firth of the Forth, Scotland *British Geological Survey Open Report* OR/18/016: 1–49.
- Pearson EJ, Juggins S, Talbot HM *et al.* 2011. A lacustrine GDGT-temperature calibration from the Scandinavian Arctic to Antarctic: renewed potential for the application of GDGT-paleothermometry in lakes. *Geochimica et Cosmochimica Acta* **75**: 6225–6238.
- Pfennig N. 1977. Phototrophic green and purple bacteria: a comparative, systematic survey. *Annual Review of Microbiology* **31**: 275–290.
- Powers L, Werne JP, Vanderwoude AJ *et al.* 2010. Applicability and calibration of the TEX₈₆ paleothermometer in lakes. *Organic Geochemistry* **41**: 404–413.
- Poynter J, Eglinton G 1990. Molecular composition of three sediments from hole 717c: the Bengal Fan *Proceedings of the Ocean Drilling Program, Scientific Results*, 116: 155–161.
- Prahl FG, Wakeham SG. 1987. Calibration of unsaturation patterns in long-chain ketone compositions for palaeotemperature assessment. *Nature* **330**: 367–369.
- Rollins HB, Carothers M, Donahue J. 1979. Transgression, regression and fossil community succession. *Lethaia* **12**: 89–104.
- Ronkainen T, McClymont EL, Välranta M *et al.* 2013. The *n*-alkane and sterol composition of living fen plants as a potential tool for palaeoecological studies. *Organic Geochemistry* **59**: 1–9.
- Saesaengseerung N 2013 *High-throughput methods for the analysis of pigments in aquatic sediments*. PhD Thesis, University of York.
- Scheer H. 1991. Structure and occurrence of chlorophylls. In *Chlorophylls*, Scheer H (ed). CRC Press: Boca Raton; 3–30.
- Schouten S, Hopmans EC, Schefuß E *et al.* 2002. Distributional variations in marine crenarchaeotal membrane lipids: a new tool for reconstructing ancient sea water temperatures? *Earth and Planetary Science Letters* **204**: 265–274.
- Schouten S, Hopmans EC, Sinninghe Damsté JSS. 2013. The organic geochemistry of glycerol dialkyl glycerol tetraether lipids: a review. *Organic Geochemistry* **54**: 19–61.
- Schouten S, Huguet C, Hopmans EC *et al.* 2007. Analytical methodology for TEX₈₆ paleothermometry by high-performance liquid chromatography/atmospheric pressure chemical ionization-mass spectrometry. *Analytical Chemistry* **79**: 2940–2944.
- Selby KA, Smith DE. 2007. Late Devensian and Holocene relative sea-level changes on the Isle of Skye, Scotland, UK. *Journal of Quaternary Science* **22**: 119–139.
- Shennan I. 1989. Holocene crustal movements and sea-level changes in Great Britain. *Journal of Quaternary Science* **4**: 77–89.
- Shennan I, Horton B. 2002. Holocene land- and sea-level changes in Great Britain. *Journal of Quaternary Science* **17**: 511–526.
- Shennan I, Long AJ, Horton BP. 2015. *Handbook of Sea-Level Research*. Wiley: Chichester.
- Shuman FR, Lorenzen CJ. 1975. Quantitative degradation of chlorophyll by a marine herbivore. *Limnology and Oceanography* **20**: 580–586.
- Sidell EJ. 2003. *Holocene sea level change and archaeology in the inner Thames estuary, London, UK*. PhD Thesis, University of Durham.
- Small D, Bentley MJ, Jones RS *et al.* 2019. Antarctic ice sheet palaeo-thinning rates from vertical transects of cosmogenic exposure ages. *Quaternary Science Reviews* **206**: 65–80.
- Smith DE, Barlow NLM, Bradley SL *et al.* 2019. Quaternary sea level change in Scotland. *Earth and Environmental Science Transactions of the Royal Society of Edinburgh* **110**: 219–256.
- Squier AH, Hodgson DA, Keely BJ. 2002. Sedimentary pigments as markers for environmental change in an Antarctic lake. *Organic Geochemistry* **33**: 1655–1665.
- Sun D, Tan W, Pei Y *et al.* 2011. Late Quaternary environmental change of Yellow River Basin: an organic geochemical record in Bohai Sea (North China). *Organic Geochemistry* **42**: 575–585. <https://doi.org/10.1016/j.orggeochem.2011.04.011>
- Tierney JE, Russell JM. 2009. Distributions of branched GDGTs in a tropical lake system: implications for lacustrine application of the MBT/CBT paleoproxy. *Organic Geochemistry* **40**: 1032–1036.
- Tierney JE, Russell JM, Eggemont H *et al.* 2010. Environmental controls on branched tetraether lipid distributions in tropical East African lake sediments. *Geochimica et Cosmochimica Acta* **74**: 4902–4918.
- van Soelen EE, Lammertsma EI, Cremer H *et al.* 2010. Late Holocene sea-level rise in Tampa Bay: integrated reconstruction using biomarkers, pollen, organic-walled dinoflagellate cysts, and diatoms. *Estuarine, Coastal and Shelf Science* **86**: 216–224.
- Volkman JK. 1986. A review of sterol markers for marine and terrigenous organic matter. *Organic Geochemistry* **9**: 83–99.
- Volkman JK. 2005. Sterols and other triterpenoids: source specificity and evolution of biosynthetic pathways. *Organic Geochemistry* **36**: 139–159.
- Walker JS, Squier AH, Hodgson DA *et al.* 2002. Origin and significance of 13²-hydroxychlorophyll derivatives in sediments. *Organic Geochemistry* **33**: 1667–1674.
- Wang C, Bendle J, Yang Y *et al.* 2016. Impacts of pH and temperature on soil bacterial 3-hydroxy fatty acids: development of novel terrestrial proxies. *Organic Geochemistry* **94**: 21–31.
- Wanner H, Beer J, Bütikofer J *et al.* 2008. Mid- to Late Holocene climate change: an overview. *Quaternary Science Reviews* **27**: 1791–1828.
- Weijers JWH, Schouten S, van den Donker JC *et al.* 2007. Environmental controls on bacterial tetraether membrane lipid distribution in soils. *Geochimica et Cosmochimica Acta* **71**: 703–713.
- Wilson MA, Airs RL, Atkinson JE *et al.* 2004. Bacterioviridins: novel sedimentary chlorins providing evidence for oxidative processes affecting palaeobacterial communities. *Organic Geochemistry* **35**: 199–202.
- Yang Y, Wang C, Bendle JA *et al.* 2020. A new sea surface temperature proxy based on bacterial 3-hydroxy fatty acids. *Geochemistry* **141**: 1–15.
- Zech M, Krause T, Meszner S *et al.* 2013. Incorrect when uncorrected: reconstructing vegetation history using *n*-alkane biomarkers in loess-paleosol sequences – A case study from the Saxonian loess region, Germany. *Quaternary International* **296**: 108–116.
- Zhu C, Wagner T, Talbot HM *et al.* 2013. Mechanistic controls on diverse fates of terrestrial organic components in the East China Sea. *Geochimica et Cosmochimica Acta* **117**: 129–143.